

Axonal Transport of Mitochondria to Synapses Depends on Milton, a Novel *Drosophila* Protein

R. Steven Stowers,^{2,4} Laura J. Megeath,^{1,4}
Jolanta Górska-Andrzejak,^{3,6}
Ian A. Meinertzhagen,³ and Thomas L. Schwarz^{1,4,5}

¹Division of Neuroscience
Children's Hospital
Enders 208

300 Longwood Avenue
Boston, Massachusetts 02115

²Department of Molecular and Cell Biology
University of California, Berkeley
Life Sciences Addition
Room #548

Berkeley, California 94720

³Life Sciences Centre
Dalhousie University
Halifax, Nova Scotia B3H 4J1
Canada

⁴Department of Molecular and Cellular Physiology
Stanford School of Medicine
Beckman Center
Stanford, California 94305

Summary

A protein required to localize mitochondria to *Drosophila* nerve terminals has been identified genetically. Photoreceptors mutant for *milton* show aberrant synaptic transmission despite normal phototransduction. Without Milton, synaptic terminals and axons lack mitochondria, although mitochondria are numerous in neuronal cell bodies. In contrast, synaptic vesicles continue to be transported to and concentrated at synapses. Milton protein is associated with mitochondria and is present primarily in axons and synapses. A likely explanation of the apparent trafficking defect is offered by the coimmunoprecipitation of Milton and kinesin heavy chain. Transfected into HEK293T cells, Milton induces a redistribution of mitochondria within the cell. We propose that Milton is a mitochondria-associated protein required for kinesin-mediated transport of mitochondria to nerve terminals.

Introduction

The synaptic terminals of neurons invariably contain mitochondria (Peters et al., 1991). In addition to providing ATP, these mitochondria likely help buffer local Ca²⁺ concentrations in some nerve terminals (Werth and Thayer, 1994), and this Ca²⁺ buffering by mitochondria has been implicated in synaptic plasticity (reviewed in Zucker 1999). The considerable distances that can separate a terminal from its cell body present to neurons an extreme case of a general requirement: the need to place the means of ATP production near the site of demand

so that the slow diffusion of ATP does not limit the function of the cell. To this end, mitochondria can move within the cell, altering their distribution in response to changes in the local energy state (Wong-Riley and Welt, 1980; Hollenbeck, 1996).

The mechanism by which mitochondria distribute themselves appropriately within the cell remains obscure, but is certain to involve axonal transport in neurons. Actins, microtubules, kinesins, and dyneins have each been implicated in mitochondrial motility (Nangaku et al., 1994; Langford, 1995; Pereira et al., 1997; Tanaka et al., 1998; Ligon and Steward, 2000; reviewed in Hollenbeck, 1996; Goldstein and Yang, 2000). In locust photoreceptors, for example, mitochondria move radially toward the phototransducing organelle, the rhabdome, during adaptation to light, and this motility is blocked by reagents that perturb actin polymerization (Stürmer et al., 1995). On the other hand, the association of particular isoforms of kinesin (KIF1B, KLP67A, KIF5B) with the mitochondrion implicates microtubule-based transport (Nangaku et al., 1994; Peirira et al., 1997; Tanaka et al., 1998). In the case of axonal transport of mitochondria, there is evidence implicating both of these mechanisms. It has been suggested, based on pharmacological and imaging studies, that mitochondria are primarily dependent on kinesins for anterograde and dyneins for retrograde transport (reviewed in Hollenbeck, 1996; Ligon and Steward, 2000). In *Drosophila*, mutations in the conventional kinesin heavy chain gene (*khc*) cause swellings of the axon that are filled with various organelles, including mitochondria (Hurd and Saxton, 1996). Interestingly, a mutation in one kinesin has recently been linked to a peripheral neuropathy that has an underlying defect in axonal transport (Zhao et al., 2001).

We have carried out a genetic screen for *Drosophila* mutations that affect the cell biology of the axon and its synaptic terminal. From this screen, we have identified a protein, which we call Milton, that is crucial to the proper localization of mitochondria within neurons.

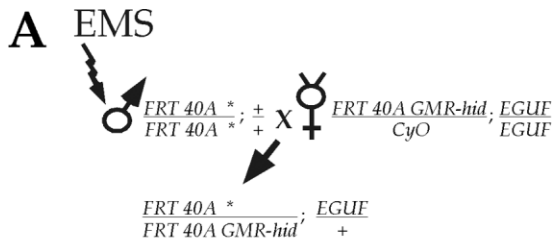
Results

A Genetic Screen Identifies a Mutant with Impaired Synaptic Transmission

To identify previously unknown genes required for axonal and synaptic function, we have carried out a genetic screen in *Drosophila*. Screens for this class of mutation can be hindered because a mutation in an essential protein may be lethal at embryonic or early larval stages and, from the vast number of such early lethal mutations in *Drosophila*, it is difficult to select those that pertain directly to axon outgrowth, axonal transport, synapse formation, or synaptic function. Our genetic screen (Figures 1A and 1B) recognized the desired mutants on the basis of defective photoreceptor function and was enabled by a genetic technique that produces flies whose eyes are entirely homozygous for a single mutant genotype, although the other tissues of those flies remain heterozygous (Stowers and Schwarz, 1999). Thus,

⁵ Correspondence: thomas.schwarz@tch.harvard.edu

⁶ Current address: Institute of Zoology, Jagiellonian University, Ingardena 6, 30-060 Kraków, Poland.



B

Generation	Selection Criteria
F1	aberrant phototaxis
F2	aberrant phototaxis
F2	no "on/off" transient electroretinogram

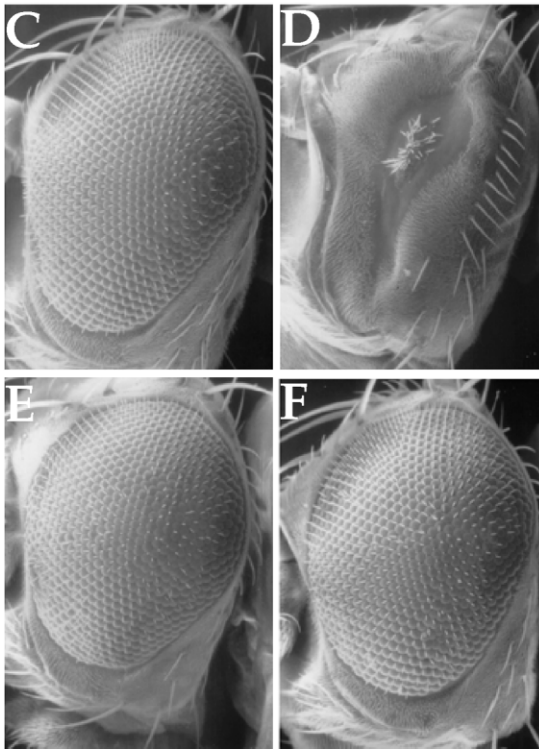


Figure 1. Mutagenesis Scheme

(A) EMS mutagenized males with an isogenized *FRT40A* chromosome were mated as shown to produce progeny whose eyes contain exclusively a single mutagenized 2L chromosome. Homozygous mutant recessive eye phenotypes are revealed in this F₁ generation. (B) Outline of the selection criteria. In the F₁ generation, recombinant-eye flies showing aberrant phototactic behavior were selected for mating. In the F₂ generation, recombinant-eye progeny showing aberrant phototaxis were further analyzed by electroretinogram (ERG), and those with reductions in the on- and off-transients were saved.

(C–F) Scanning electron micrographs of fly eyes. (C) Wild-type. (D) *yw; FRT40A GMR-hid 2L CL/CyO; EGUF/EGUF*. (E) *yw; FRT40A GMR-hid 2L CL/FRT40 parental; EGUF/+*. (F) *yw; FRT40A GMR-hid 2L CL/FRT40A *mitl*⁹²; EGUF/+*. The dominant photoreceptor-specific cell lethality of *GMR-hid*, shown in (D), can be suppressed by mitotic recombination (E). The external morphology of a homozy-

gous fly with a mutation in an essential gene remains viable, albeit blind. This technique employs the GAL4/UAS and FLP/FRT systems (Brand and Perrimon, 1993; Xu and Rubin, 1993) to induce mitotic recombination of FRT-bearing chromosome arms specifically in the eye by means of an eye-specific GAL4 driver in combination with a UAS-FLP transgene. The dominant, photoreceptor-specific, cell-lethal transgene *GMR-hid* is used to eliminate all photoreceptors in which the desired chromosome arm has not been made homozygous. In the absence of mitotic recombination in flies possessing even a single copy of a *GMR-hid* transgene, all photoreceptors are eliminated during development through programmed cell death (Figures 1C and 1D). In this genetic screen, photoreceptor neurons may only become viable by losing *GMR-hid* through mitotic recombination, but in the process they must become homozygous for the homologous (mutagenized) chromosome. Two key features make this screen especially powerful. (1) The mutant phenotype is recognized in the F₁ generation, facilitating high-throughput selection of candidate mutations, and (2) mutations in essential genes can be recovered because the mutation is homozygous solely in the eye.

We exploited the phototactic behavioral response of *Drosophila* for the primary screen of F₁ generation flies whose eyes were exclusively homozygous for the mutagenized chromosome. Flies that failed to move appropriately toward the light were individually mated and retested in the next generation to determine the heritability of the visual defect. Because the eyes alone were homozygous for the mutation, extraneous mutations, such as those affecting muscles or higher visual centers, did not cause false positives. As a secondary screen, the electrical responses to a light flash were evaluated from the electroretinogram (ERG) in F₂ flies. ERGs have two discriminable components, a sustained negative response that arises from phototransduction (Heisenberg, 1971) and on- and off-transients that correlate with synaptic transmission to second-order cells of the first neuropile or lamina (Coombe, 1986). Consequently, mutants could be selected with a preferential reduction in on- and off-transients; the defect in such mutants, therefore, would likely lie in events subsequent to phototransduction. A summary of the screen is presented in Figures 1A and 1B.

From ~3000 lethal mutations screened, 24 mutants representing 14 lethal complementation groups on chromosome arm 2L were identified. The eyes of 12 of these complementation groups appeared, to varying extents, either roughened or reduced in size. These complementation groups were given a lower priority because they more likely involved developmental defects or defects in housekeeping genes. For two complementation groups, however, homozygous mutant eyes were indistinguishable in their external morphology from eyes homozygous for the parental (premutagenized) chromosome (Figures 1E and 1F). One of these groups, represented by two alleles, corresponded to *synaptotagmin* (*syt*) as determined by complementation tests with existing *syt*

gous *mitl*⁹² recombinant eye is phenotypically normal (F) and is indistinguishable from the parental chromosome recombinant eye (E).

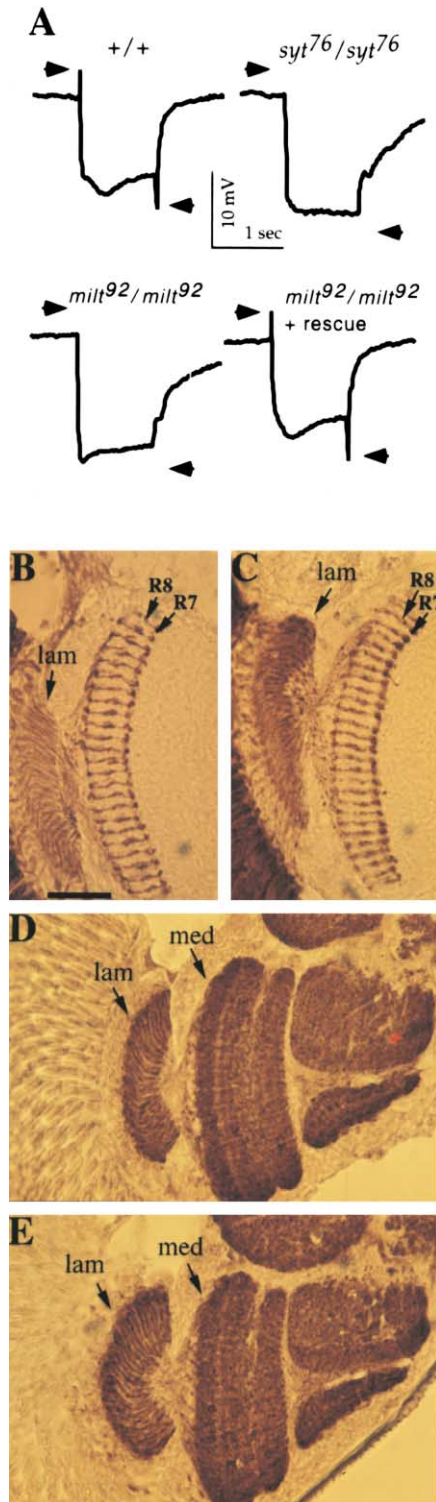


Figure 2. Milton Disrupts Photoreceptor Synaptic Transmission, but Not Phototransduction or Photoreceptor Morphology

(A) *milton* mutants lack ERG on- and off-transients, indicating a synaptic transmission defect. Transients (arrows) are present when the control chromosome (+/+) is made homozygous in the genotype *yw; FRT40A GMR-hid 2L CL/FRT40A parental; EGUF/+*, but lacking when either *synaptotagmin* (*syt⁷⁶/syt⁷⁶*) or *milton* (*milt⁹²/milt⁹²*) are made homozygous in genotypes: *yw; FRT40A GMR-hid 2L CL/FRT40A syt⁷⁶; EGUF/+*, and *yw; FRT40A GMR-hid 2L CL/FRT40A*

alleles. Our recovery of alleles of *syt*, for which an effect on neurotransmitter release is well established, validates our screening method for identifying genes required for synaptic and axonal function. The other complementation group was mapped to cytological region 27CD by complementation tests with deletion mutants on chromosome arm 2L, including *Df(2L) J-H*. This previously unidentified gene was named *milton* (*milt*) (after the blind British poet). Two P element alleles from the Berkeley *Drosophila* Genome Project, *l(2) K06704* and *l(2) K14514* (hereafter *milt^{t(2) K06704}* and *milt^{t(2) K14514}*), failed to complement our two EMS alleles *milt⁹²* and *milt¹⁸⁶*.

Although homozygous *milt⁹²* and *milt¹⁸⁶* eyes showed no external morphological defect (Figure 1F), the ERG revealed a clear physiological defect: the on- and off-transients that report the synaptic activation of second-order cells were missing (Figure 2A). This phenotype is identical to that of a *synaptotagmin* allele similarly made homozygous in the eye and is likely to reflect a severe alteration in transmission at the photoreceptor terminals. This defect cannot be attributed to the recombination and cell death that occurs in the process of making the eye homozygous by the *EGUF/hid* method because the ERG of recombinant eyes homozygous for the control parental chromosome does not lack on- and off-transients. The generally robust sustained negative component of the *milt* ERG indicates, moreover, that the photoreceptors generate a light-evoked response but that this signal is not communicated to the postsynaptic cells.

To determine if the *milt* ERG phenotype can be explained by a gross structural or developmental defect, sections of heads from flies with either control parental or *milt⁹²* recombinant eyes were labeled with antibodies to Chaoptin, to label photoreceptor axons, or to Synaptotagmin, to label synaptic vesicles (Figures 2B–2E). No alteration was observed in the regular array of R7 or R8 photoreceptor axons that project into the medulla, nor were there any obvious abnormalities in the shape of the lamina, although the high density of axons from R1–R6 photoreceptors that innervate this neuropile precludes following individual axons. These findings do not exclude the possibility of a subtle misrouting of the mu-

milt⁹²; EGUF/+. In *milt⁹²/milt⁹² + rescue*, a *milton* genomic rescue construct on the X chromosome is also present and the on- and off-transients are restored.

(B–E) Horizontal head sections of recombinant-eye flies immunolabeled with the photoreceptor axonal marker mAb24B10 (B and C), a photoreceptor-specific antibody against Chaoptin (Fujita et al., 1982), or the synaptic vesicle marker syt (D and E). R1–R6 and R7–R8 axonal projections to the lamina and medulla, respectively, are morphologically indistinguishable between *parental* (B) and *milt⁹²/milt⁹²* (C) photoreceptors. No differences are observed in synaptic vesicle localization or neuropile morphology in the lamina or medulla between the *parental* (D) and *milt⁹²/milt⁹²* (E) recombinant eyes. In these head sections of recombinant eyes, the lamina and medulla contain both homozygous mutant photoreceptor synapses and heterozygous (phenotypically wild-type) nonphotoreceptor synapses. From these immunolabelings we conclude that gross morphological defects do not underlie the lack of on- and off-transients in the mutant. Genotypes: *yw; FRT40A GMR-hid 2L CL/FRT40A parental; EGUF/+*. (B and D); *yw; FRT40A GMR-hid 2LCL/FRT40A milt⁹²; EGUF/+* (C and E). Abbreviations: Lam, lamina; Med, medulla. Scale bar: 50 μm.

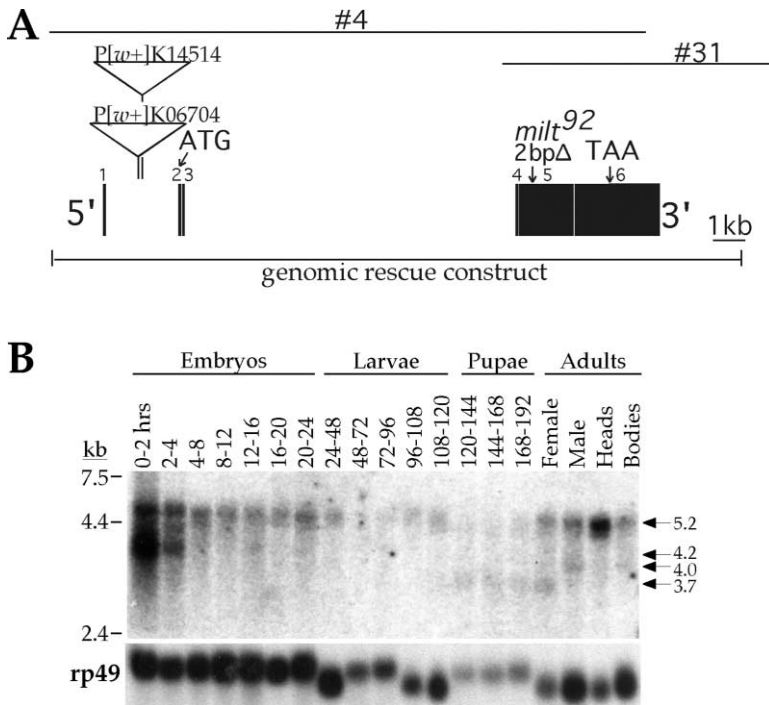


Figure 3. Milton Cloning and Expression

(A) An alignment of the six exons of *milton* (black boxes), genomic phage clones (above), and rescue construct (below). The start codon in exon 2 and stop codon in exon 6 are indicated as are the location of the 2 bp deletion at amino acid 348 in *milt*⁹² and the insertion sites of P elements in *milt*^{(2) K06704} and *milt*^{(2) K14514}. In addition to the 5.2 kb cDNA, a second class of cDNAs was recovered that exhibited an alternative polyadenylation site at nucleotide 4262 that does not alter the predicted Milton protein sequence.

(B) *milton* mRNA transcripts from wild-type Canton-S flies (staged in hours after egg laying at 25°C) probed with the 5.2 kb cDNA. Four distinct transcripts sizes are observed. Below, the same blot reprobred with rp49.

tant photoreceptor axons. Photoreceptors contribute most of the presynaptic active zones in the lamina (Meinertzhagen and O'Neil, 1991; Meinertzhagen and Sorra, 2001) and a smaller subset of the medulla synapses. When the photoreceptors were homozygous for *milton*⁹², both of these neuropiles labeled heavily with Synaptotagmin, suggesting that synapses had formed and synaptic vesicles had been concentrated in the terminals, which we later addressed in detail by electron microscopy (see below). This initial characterization of *milton* suggested that in photoreceptors, the gene is involved in a physiological process occurring after phototransduction and necessary for proper synaptic function.

milton Function Is Not Restricted to Photoreceptors

*milt*⁹²/*milt*⁹², *milt*⁹²/*Df(2L) J-H*, *milt*¹⁸⁶/*milt*⁹², and *milt*¹⁸⁶/*Df(2L) J-H* animals do not attain the third larval instar. Animals of each of these genotypes hatch from their egg cases and, if selected as homozygotes at 24–36 hr and cultured in uncrowded conditions separated from their heterozygous siblings, typically survive for 3–5 days. Although the *milton* mutants showing the greatest longevity were old enough to have attained the third larval instar, none were, in fact, observed to progress beyond the second instar. Larvae of these genotypes were sluggish but exhibited robust withdrawal responses when poked. The lethal phase and phenotype of *milt*⁹²/*milt*⁹² and *milt*⁹²/*Df(2L) J-H* animals are indistinguishable and *milt*⁹² is therefore likely a null allele. This was subsequently confirmed by molecular characterization (see below). *milt*^{(2) K06704} and *milt*^{(2) K14514} homozygotes die as adults and are thus hypomorphic *milton* alleles. Newly eclosed *milt*^{(2) K06704} and *milt*^{(2) K14514} adult homozygotes can live at least a week, but scarcely move, right themselves with great difficulty when overturned, and

more typically, die soon after eclosion. These generalized neurological defects and the early lethality of the null alleles indicate that *milton* function is not restricted to the photoreceptors.

Molecular Cloning and Developmental Expression of the *milton* Gene

Cloning of the gene corresponding to the *milt* complementation group was facilitated by the *milt*^{(2) K06704} and *milt*^{(2) K14514} P element alleles. Plasmid rescue of the *milt*^{(2) K06704} P element was performed, and 5.5 kb of genomic DNA adjacent to its insertion site was recovered. This genomic fragment was used as a hybridization probe to isolate genomic phage from the region. Genomic Southern analysis indicated that the location of the *milt*^{(2) K14514} P element insertion site was ~100 bp from that of *milt*^{(2) K06704} (data not shown). A ~7 kb EcoRI/Sall genomic fragment from phage #4 (Figure 3A) spanning the P element insertion sites of both *milt*^{(2) K06704} and *milt*^{(2) K14514} was used as a hybridization probe against the 0–24 hr LD embryonic cDNA library. A 5.2 kb candidate cDNA was recovered that was determined to hybridize to genomic DNA on both sides of the *milt*^{(2) K06704} and *milt*^{(2) K14514} insertion sites. This cDNA was sequenced in its entirety, as were the entire corresponding protein coding regions of genomic DNA from the *milt*⁹²/*milt*⁹² and *milt*¹⁸⁶/*milt*¹⁸⁶ mutants. This analysis surprisingly revealed an identical 2 bp deletion not present in the isogenized parental chromosome but present in both the *milt*⁹² and *milt*¹⁸⁶ chromosomes even though the alleles were isolated independently from one another (Figure 3A, exon 5 arrow and Figure 4). This mutation introduces a frame shift in the coding region (Figure 3A) that precludes the translation of two-thirds of the predicted protein. The two P element alleles were inserted into the first intron of this transcription unit. Further evidence supporting



Figure 4. Milton Aligned with Human Homologs and with HuHAP-1

The predicted coiled-coil domain of Milton is indicated by the dotted line, and the region of HuHAP-1 that is known to bind to Huntingtin and Dynactin is indicated by the solid line. The strongest homology of the four proteins lies toward the beginning of the coiled-coil domain, but some conservation is found in the Huntingtin and Dynactin binding region as well. The accession numbers are: huMilt1-Genpept-BAA82994 (Kikuno et al., 1999), huMilt2 Genpept-BAA25475 (Nagase et al., 1998), and HuHAP1-Swissprot-P54255 (Li et al., 1995).

the supposition that the gene contained in the 5.2 kb cDNA corresponds to *milton* was obtained with a rescue construct containing 22 kb of genomic DNA that extends from ~1.5 kb upstream to ~2.5 kb downstream of the furthest 5' and 3' sequences present in the 5.2 kb cDNA (Figure 3A). This construct contains no other predicted genes and fully rescues both the ERG phenotype (Figure 2A) and the lethality of *milt⁹²* (data not shown). This result, together with both the sequence changes between the *milt⁹²* and parental chromosomes and the location of the P elements, demonstrates that the identified 5.2 kb cDNA indeed represents the *milton* transcript.

The temporal expression pattern of *milt* mRNA during development is shown in Figure 3B. Although the pattern and level of their expression vary considerably, at least four different *milt* transcripts can be distinguished, including mRNAs of 5.2, 4.2, 4.0, and 3.7 kb (Figure 3B). *milt* transcripts are enriched in adult heads as compared with bodies, consistent with their enrichment in neurons. The presence of transcripts in early embryos prior to the onset of neurogenesis would suggest, however, that *milton* also functions outside the nervous system. The abundance of transcripts in 0–2 hr embryos in particular suggests that some *milt* transcript is maternally deposited. The lethal phases of *milt⁹²/milt⁹²* homozygous animals derived from mothers with either *milt⁹²/milt⁹²* or *milt⁹²/CyO*, *y+* germlines were indistinguishable, indicating that maternally contributed transcripts are not essential for the viability of these larvae and do not significantly alleviate the defects that ultimately kill the organism. Thus, although *milt* transcripts are present from the start of embryogenesis, their absence does not prove lethal until the first and second instar.

The Predicted Milton Protein

The 5.2 kb *milton* cDNA encodes a predicted protein of 1116 amino acids. Seven other embryonic cDNAs that were examined had the same open reading frame. Sequence analysis did not indicate a transmembrane domain. Amino acids 140 to 380 are, however, likely to form a lengthy coiled-coil domain that includes a leucine zipper. Database searches provide some additional insights. Two uncharacterized human brain cDNAs of high homology were identified, KIAA1042 (Kikuno et al., 1999), hereafter called huMilt1, and KIAA0549 (Nagase et al., 1998), hereafter called huMilt2. These have 30% and 28% overall identity, respectively, with the predicted Milton protein (Figure 4). Only a single *milton* gene is predicted in the *Drosophila* genome. Milton, huMilt1, and huMilt2 share two regions of particular homology. The most amino-terminal of these regions (aa 66–165) is 100 amino acids in length and 60% identical to huMilt1. This region of the Milton protein also shows homology, but with only 20%–25% identity, to paramyosins from several different species. This region is followed by the remainder of the predicted coiled-coil domain. Over this portion of the coiled-coil, Milton shows 36% identity to huMilt1 and ≤26% identity to a family of proteins with coiled-coil structures, including myosins, and tropomyosins. It is the coiled-coil tail regions of these proteins to which Milton shows homology, not the head, or ATPase motor domains. The tail regions of these proteins are believed to mediate dimerization,

subcellular localization, and other protein-protein interactions (reviewed in Vallee and Sheetz, 1996). The second region of high identity between Milton and both huMilt1 (47%) and huMilt2 (40%) is in the carboxy half of the protein (aa 670–720). This domain is not found in any other protein in the database and, so, the functional significance of the conservation of this region remains to be determined.

Database searches of mammalian genomes revealed an additional homology: Huntingtin-associated protein, HAP-1, a protein identified on the basis of its binding to the Huntingtin protein (Li et al., 1995). Though not as closely related to Milton as are the huMilt proteins, the homology is extensive (Figure 4), with >50% identity to the Milton proteins for a 60 amino acid region at the N terminus of the predicted coiled coil. No other protein in the *Drosophila* genome shows greater homology to HAP-1 than Milton; thus HAP-1 does not have a closer homolog in the fly. The function of HAP-1 is not known, but it associates with membrane-bound organelles within neurons, undergoes rapid axonal transport, and binds to p150/Glued, a member of the dynactin complex that functions in retrograde transport. Interestingly, amino acids 323–416 of HAP-1 are sufficient for its interaction with huntingtin and p150/Glued (Li et al., 1998), and this region shows significant homology with Milton.

Biochemical Characterization of Milton Protein

To understand better the cellular function of Milton, we began a biochemical analysis and determined its distribution within the cell by subcellular fractionation. To this end, we first generated antisera and monoclonal antibodies to each of four nonoverlapping Milton fusion proteins (Figure 5A; Experimental Procedures). On immunoblots of *Drosophila* head extracts, four bands of 120–160 kd were observed in general agreement with the predicted MW of Milton (120 kd). All four bands are recognized by monoclonal antibodies 2B30, 2A108, 4A75, and 5A124, the epitopes of which map to three distinct regions of the Milton protein (Figure 5A), indicating that each band is indeed Milton and not spurious cross-reactivity. The identification of these bands as Milton was further confirmed on immunoblots on which protein from 20–24 hr embryos of either *milt⁹²/milt⁹²* or control animals were compared using monoclonal antibody 4A75. All four bands were absent from the mutant embryos (Figure 5B). One polyclonal antiserum, P1-152, recognized only one of the four Milton bands. This antiserum is directed against the amino-terminal region of the protein; thus, apparently, part of this region is absent from some of the smaller isoforms of the protein. The differences between the isoforms are not known.

Sucrose gradient fractionation determined that Milton is likely to be associated with mitochondria. Milton and the mitochondrial marker cytochrome c comigrate precisely on these gradients (Figure 5D). In contrast, Milton did not cosediment on 5%–25% glycerol gradients with Csp, a synaptic vesicle marker, and Milton barely overlapped the sedimentation profile of the plasma membrane marker Syntaxin on either glycerol (Figure 5C) or OptiPrep gradients (data not shown). Thus, under these conditions, little if any Milton stably associated with synaptic vesicle or plasma membrane fractions; rather, most comigrated with mitochondria.

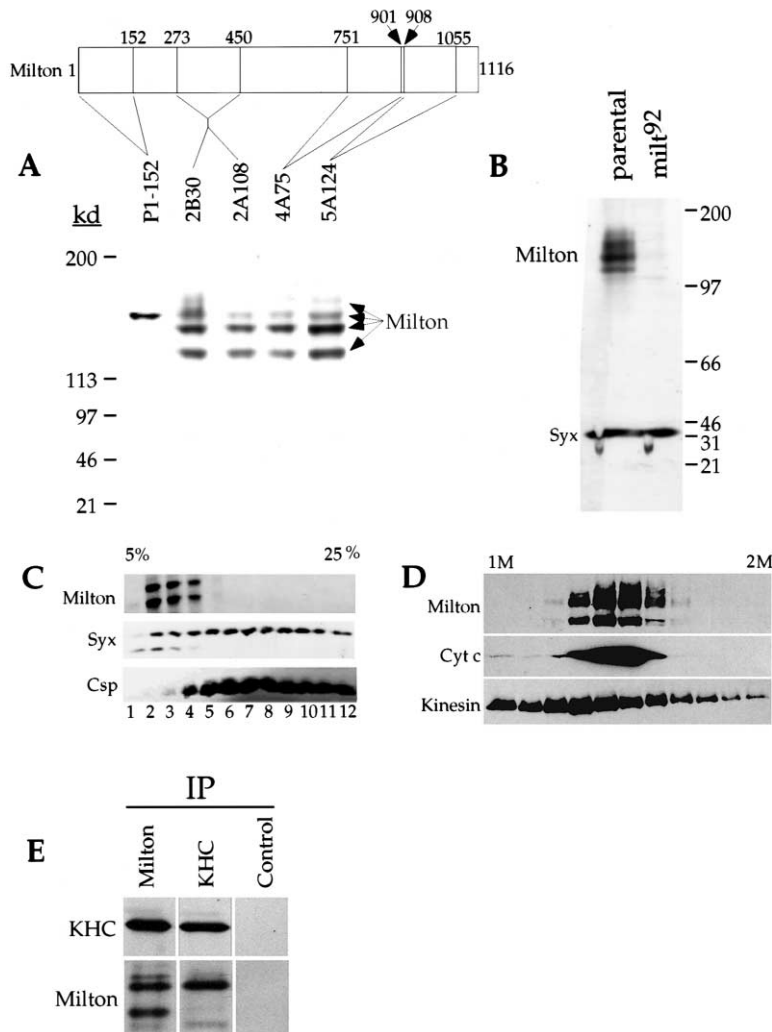


Figure 5. Milton Associates with Mitochondria and Kinesin Heavy Chain

(A) Epitope map of anti-Milton antibodies and Milton protein in head extracts. P1-152 is an affinity purified polyclonal, while all others are monoclonal antibodies. The immunogen for each antibody is indicated above. Four distinct Milton proteins between 120 and 160 kd are recognized by each monoclonal, while the amino-terminal polyclonal recognizes a single isoform of approximately 150 kd. (B) Using 4A75, the same four Milton bands are observed in 20–24 hr wild-type embryos, but not in *mult⁹²/mult⁹²*. The blot was simultaneously probed with anti-Syntaxin (Syx) to control for equal protein loading. (C) In 5%–25% glycerol gradient fractions of head extracts, the distribution of Milton does not correspond with synaptic vesicles (marked with Csp and Syntaxin) or plasma membrane (marked with Syntaxin). (D) The distributions of Milton and the mitochondrial marker Cyt c are indistinguishable on sucrose gradients. Kinesin heavy chain is more broadly distributed. (E) Coimmunoprecipitation of Milton and KHC. Immunoprecipitates using Milton and KHC, but not a control antibody, contain KHC (top) and Milton (bottom), although only some Milton isoforms were coprecipitated with KHC.

The subcellular localization of Milton was also examined by transfecting HEK293T cells with the *Drosophila* *milton* cDNA. Immunoreactivity, detected with any of three monoclonal antibodies to separate regions of Milton, colocalized with the mitochondrial marker MitoTracker Red (Figures 6A and 6B) with much less immunoreactivity elsewhere in the cell. No cross-reactivity of these antibodies with mammalian Milton has been detected on immunoblots (data not shown). Consistent with this finding, no Milton immunoreactivity was observed in sham-transfected cultures. Interestingly, the expression of Milton also caused a rearrangement of the mitochondria within these cells. Whereas mitochondria in sham-transfected cells were diffusely distributed within the cell, the expression of Milton induced the mitochondria to clump together in one or two large aggregates observed chiefly in the vicinity of the Golgi apparatus (Figures 6A–6D). This redistribution is discussed below. Despite the close proximity of the mitochondria and Golgi apparatus, the Golgi apparatus was often slightly separated from the mitochondria and did not appear to be associated with Milton immunoreactivity (Figure 6E). Milton was not observed on the nucleus of these cells, nor did Milton localize to recycling endo-

somes (labeled by incubation with transferrin) or to the endoplasmic reticulum (labeled with antibodies to TRAP α) (Figures 6F and 6G). Thus, Milton associates selectively with mitochondria.

To look for Milton-associated proteins, immunoprecipitates were made from *Drosophila* head extracts solubilized in 1% Triton X-100 and analyzed by SDS-PAGE and silver staining. A band was detected when either monoclonal antibody 2A108 or 5A124 was used to precipitate Milton that was absent when either of two control monoclonal antibodies were used for the precipitation. This band, which appeared somewhat larger than Milton, was excised from the gel, digested with trypsin, and analyzed by mass spectrometry. The resulting peptide masses were compared with a database of tryptic peptide masses predicted by the *Drosophila* genome and identified Kinesin heavy chain (KHC) as a likely Milton-associated protein. This was confirmed when two independent antisera to *Drosophila* KHC recognized a single band of 160 kd that comigrated with KHC in immunoprecipitates made with either monoclonal antibody 2A108 or 5A124; two control antibodies did not precipitate KHC (Figure 5E). In contrast, the Milton immunoprecipitates did not contain immunoreactivity for the retro-

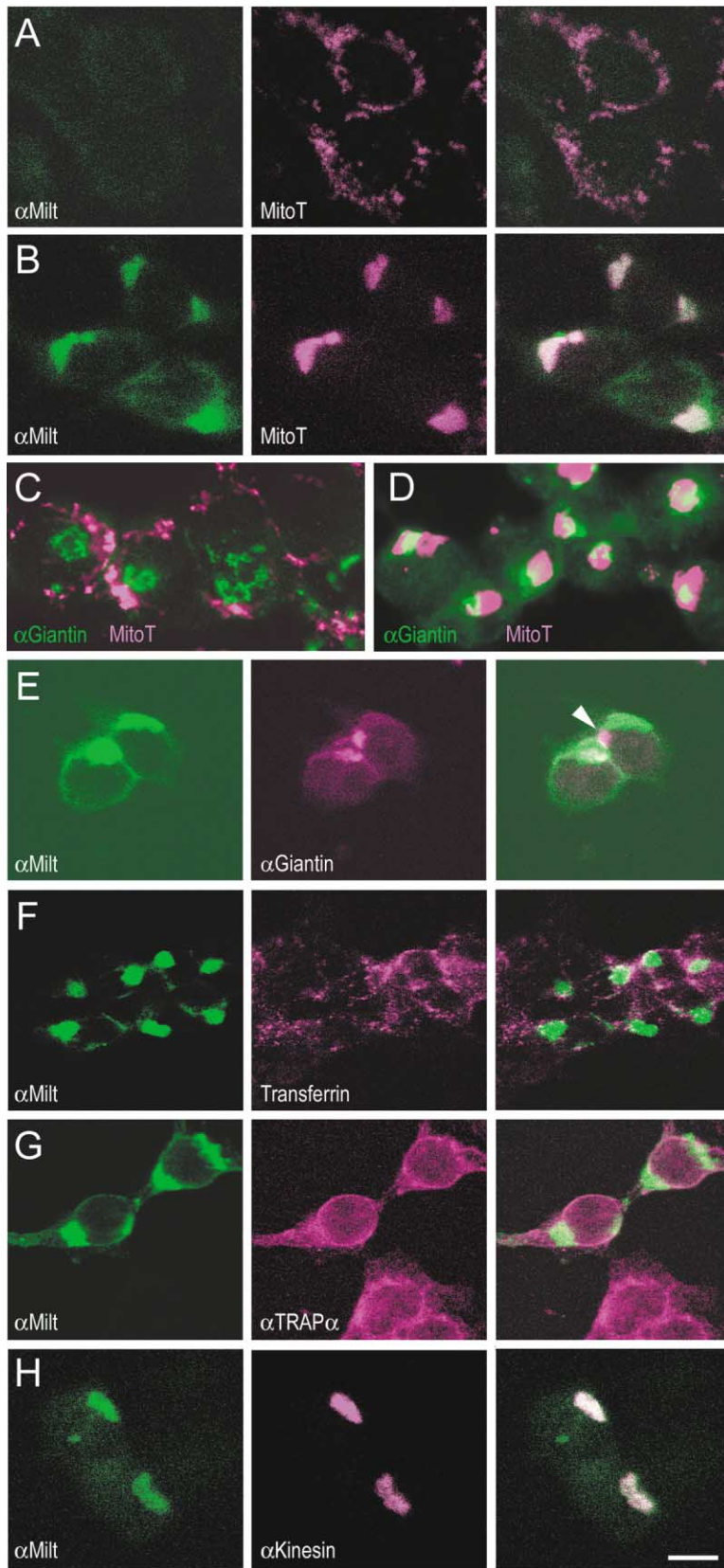


Figure 6. Milton Selectively Colocalizes with Mitochondria in HEK293T Cells

(A and B) Milton mAb 2A108 labeling corresponds to mitochondria labeled with MitoTracker Red in transfected cells (B), but not sham-transfected controls (A). Mitochondria are diffusely distributed in sham-transfected cells (A and C) but in milton-transfected cells (B and D) form tight aggregates near the Golgi (visualized with antibodies to giantin). (E) Labeling with antibodies to Milton and giantin suggests the Golgi itself may not contain Milton (arrowhead). Milton did not colocalize with transferrin AlexaFluor 594 (F) or anti-TRAP α (G), markers for endosomes and endoplasmic reticulum, respectively. (H) Milton colocalizes with Kinesin, labeled with a polyclonal anti-kinesin antibody. Scale bar, 10 μ m.

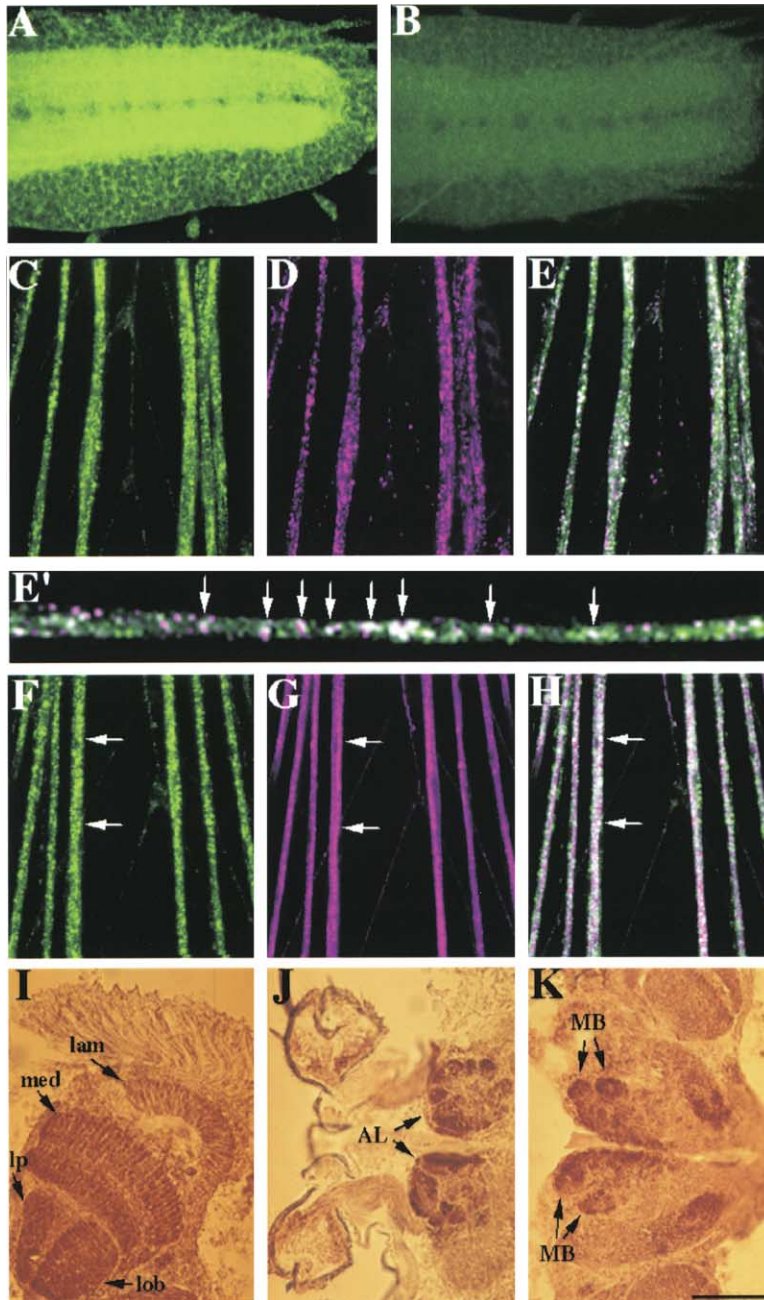


Figure 7. Milton Is Expressed in Axonal and Synaptic Regions and Colocalizes with Mitochondria and KHC

(A) Ventral ganglion from a *milton*^{+/+} first instar larva labeled with mAb 2A108. The synaptic region is highly immunoreactive, with sparser signals in cell bodies.

(B) Immunoreactivity was not observed in *milt*⁹²/*milt*⁹² larva, demonstrating the specificity of the antibody.

(C–E) Peripheral nerves from *milton*^{+/+} first instar larva immunolabeled with mAb2A108 (C) or mitochondria marker Hsp60 (D), their overlay (E), and a higher magnification thereof (E'). Milton and Hsp60 both exhibit punctate expression in peripheral nerves. Many of the puncta coincide, with most of the mitochondria associated with Milton immunoreactivity (arrows).

(F–H) Peripheral nerves from first instar larva immunolabeled with mAb 2A108 (F) or KHC (G) and their overlay (H). Milton and KHC expression overlap in places (arrows) though KHC distribution is more widespread.

(I) Optic lobes labeled with 2A108. All synaptic regions are immunoreactive.

(J and K) The central brain region of an adult head labeled with mAb 5A124 (J) and mAb 2A108 (K). Immunoreactivity is present in all synaptic regions but is particularly high in the antennal lobe and mushroom bodies (arrows). Abbreviations: lam, lamina; med, medulla; lob, lobula; lp, lobula plate; MB, mushroom body; AL, antennal lobe.

Scale bar: 63.5 μ m in (A) and (B), 40 μ m in (C)–(H), and 100 μ m in (I)–(K).

grade motor dynein. In complementary Western blots, Milton was detected in immunoprecipitates made with a KHC antiserum. Intriguingly, not all Milton isoforms appeared to associate equally with KHC (Figure 5E). Together, the coimmunoprecipitation and mass spectrometry experiments indicate that Milton is associated with KHC. The distribution of Kinesin and Milton in transfected HEK293T cells also heavily overlapped (Figure 6H), consistent with such an association.

Milton Colocalizes with Mitochondria in Axons and Synapses

The association of Milton with both mitochondria and KHC suggested a role for this protein in the axonal trans-

port of mitochondria. To explore this possibility further, we examined the distribution of Milton *in vivo*. One of our antibodies, Mab 2A108, showed strong immunolabeling in control but little or no labeling in *milt*⁹² animals (Figures 7A and 7B). To determine whether or not Milton and mitochondria colocalize in axons *in vivo*, first instar larva were coimmunolabeled with Mab2A108 (Figure 7C) and the mitochondria marker Hsp60 (Figure 7D). Both antibodies show a punctate labeling pattern in peripheral nerve and a large number of these puncta overlap precisely (Figure 7E). Mitochondria not labeled with Mab2A108 may be glial mitochondria not undergoing transport. Significant overlap in labeling is also observed between Mab2A108 and KHC (Figures 7F–7H), consis-

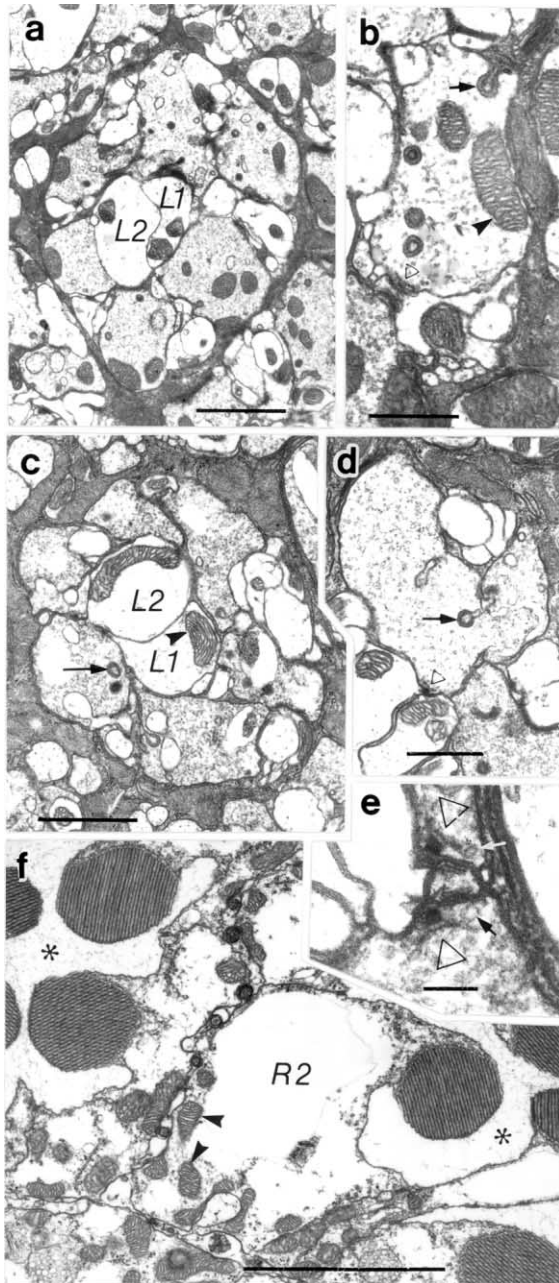


Figure 8. Mitochondria Are Absent in *milt*¹⁸⁶ Mutant Photoreceptor Terminals

(A) Cross-section of a lamina cartridge in a control fly showing the typical arrangement of two clear, monopolar cell axon profiles (L1, L2) at the cartridge axis, surrounded by the profiles of R1–R6 terminals.

(B) Typical terminal profile exhibiting diagnostic invaginations from the surrounding epithelial glia called capitate projections (arrow), tetrad synapse (open triangle), and typical mitochondria (arrowhead).

(C) Cross-section of a lamina cartridge in *milt*¹⁸⁶ of smaller size but otherwise similar composition to that in (A), with the surrounding photoreceptor terminals with capitate projections (arrow) but lacking mitochondria, contrasting with the clear mitochondrial profile in each of L2 and L1 (arrowhead).

(D) Single *milt*¹⁸⁶ terminal with clear capitate projection (arrow) and tetrad (open triangle) but lacking mitochondria.

(E) Tetrad synaptic sites (open triangles), one in each of two adjacent

terminals with the association of Milton with a portion of the cellular KHC in immunoprecipitates.

Immunolabeling was also carried out on cryostat sections of fly heads to determine the expression of Milton in the brain and optic lobes. Milton was localized primarily to neuropile, including the lamina where photoreceptors terminate (Figures 7I–7K). The strongest Milton immunoreactivity was observed in the antennal lobes and mushroom bodies, which contain high densities of terminals and axons.

Terminals of R1–R6 in *milt*¹⁸⁶ Lamina Lack Mitochondria but Have Otherwise Normal Synaptic Structures

The synaptic ultrastructure of R1–R6 terminals was examined in young flies whose photoreceptors were homozygous for either *milt*¹⁸⁶ or the control chromosome (Figure 8). Even though the retina of the compound eye sometimes had holes, suggesting that cell death occurred as a consequence of *GMR-hid* expression (see above), the underlying lamina had a regular array of modules (or cartridges). Each cartridge was apparently normal in composition, comparable in single cross-sections to those in the wild-type (Meinertzhagen and O’Neil, 1991). Their pattern even included the correct constitution of cartridges at the equator between dorsal and ventral halves of the eye (data not shown). Thus, spatial aspects of the developmental assembly of the cartridge (Meinertzhagen and Hanson, 1993; Meinertzhagen et al., 2000) seemed undisturbed. Many cartridges were smaller, however, in *milt*¹⁸⁶ than in the laminae of control or wild-type flies (Figures 8A and 8C). As in the wild-type, each *milt* cartridge had six terminals resembling those of R1–R6, surrounding the axon profiles of two monopolar cells, L1 and L2, at the cartridge axis (Figure 8C). Photoreceptor terminals homozygous for *milt*¹⁸⁶ made so-called tetrad synapses that appropriately incorporated profiles of L1 and L2 as postsynaptic elements (Figure 8) and made normal contacts with the lamina glia. The terminals also contained capitate projections, specialized invaginations from surrounding epithelial glial cells (Figures 8B and 8D).

For all their similarities, the *milt*¹⁸⁶ and *milt*⁹² terminals differed obviously from both control and wild-type terminals, however, in lacking any profiles of mitochondria (Figure 8B). No mitochondrial profiles were observed in a sample of 90 terminal profiles from *milt*¹⁸⁶ and 90 terminal profiles from *milt*⁹² flies, whereas there were 49 mitochondrial profiles in 57 terminals from parental control flies. The *milt* phenotype is thus absolute and readily detected. By contrast, photoreceptor somata in the overlying ommatidia had abundant mitochondrial pro-

*milt*¹⁸⁶ terminals, are structurally normal with a clear T-shaped presynaptic ribbon and a docked vesicle profile (arrows).

(F) Mutant photoreceptors cell bodies in the overlying compound eye, showing structurally normal microvillar rhabdomeres surrounding an extracellular space (asterisks). The cytoplasm has many obvious mitochondrial profiles (arrowheads in R2 of one ommatidium).

Scale bars: 1.0 μ m in (A),(C), and (F); 0.5 μ m in (B) and (D); and 0.1 μ m in (E).

files at densities comparable to wild-type (Figure 8F). Within the lamina, only photoreceptor terminals were bereft of mitochondria; epithelial glia and L1 and L2 neurons (which were not homozygous for the mutation) contained numerous well-preserved mitochondria, as in the wild-type (Meinertzhagen and O'Neil, 1991).

Although more subtle than the mitochondria phenotype, the density of synaptic vesicles within the terminal also differed; in *milt¹⁸⁶* the density was approximately half that of the control, a decrement that is likely secondary to the loss of mitochondria. The presence of large numbers of synaptic vesicles, but no mitochondria, indicates that loss of Milton does not generally deplete all transported organelles but that mitochondria are preferentially affected.

The selective defect in the transport of mitochondria was also confirmed in first instar larvae from which both maternally derived and zygotic Milton were absent. Whereas in control larvae, mitochondria were abundant in peripheral nerve axons and synaptic and axonal regions of the ventral ganglion, mitochondria were absent from these locations in *milt⁹²* animals (data not shown). In contrast, the distribution of the synaptic vesicle marker Synaptotagmin was indistinguishable between control and *milt⁹²* animals. Nor were axonal swellings with aggregates of mitochondria or synaptic vesicles encountered, as has been seen with partial loss of KHC function. In *milton* null larvae, the mitochondria appeared to remain entirely within the cell body of the neurons and not to enter the peripheral nerves at all. Synaptotagmin immunoreactivity was normally distributed (data not shown). Thus, Milton appears to be essential for proper axonal and synaptic localization of mitochondria but is required neither generally for axonal transport of all kinesin cargoes nor for axonal outgrowth.

Discussion

Neurons require the active transport of proteins and organelles over large distances to their terminals. Whereas synaptic vesicles are exclusively transported to the terminal, mitochondria present an additional challenge to the cell insofar as some must be sent down the axon while others are retained in the cell body. The *milton* gene is essential for the proper localization of mitochondria to the axon and terminal; in neurons homozygous for *milton*, mitochondria are restricted to the cell soma, whereas synaptic vesicles continue to enter axons and accumulate at synapses that retain normal anatomical specializations and appropriate contacts. This phenotype might arise from several mechanisms: a failure of the mitochondria to couple to the motor for transport, a failure in the regulation of the motor protein, or a failure of mitochondria to be retained in the terminal once they arrive there. Our findings are most consistent with the hypothesis that Milton acts as an adaptor protein or as part of an adaptor complex that links the appropriate kinesin motor to mitochondria. (1) Milton copurifies with mitochondria but is not observed on the plasma membrane or synaptic vesicles. (2) When expressed in HEK293T cells, Milton localizes selectively to mitochondria. (3) Milton colocalizes in vivo with a mitochondrial marker in *Drosophila* nerves. (4) Milton

and kinesin are associated with one another in immunoprecipitation experiments and colocalize in HEK293T cells. (5) Mitochondria were not observed in homozygous mutant axons; if Milton were necessary to retain mitochondria in the terminal rather than to transport them, we would expect to see numerous mitochondria in transit in the axons. (6) Overexpression of Milton in HEK293T cells disrupted the normal distribution of mitochondria within the cell. The *milton* ERG phenotype appears to result from a failure of photoreceptor neurons to transport mitochondria to the nerve terminal and not to a more general mitochondrial defect. Thus, morphologically normal mitochondria in appropriate numbers are observed in the rhabdomere region of these same photoreceptors and are likely to function properly because these cells sustain normal phototransduction.

The nature of the interactions between Milton and both mitochondria and Kinesin is not known. Milton lacks a predicted transmembrane domain and therefore may bind to a membrane protein present on the mitochondria of both *Drosophila* neurons and HEK293T cells. Although Milton and Kinesin coprecipitate, our attempts to demonstrate a direct interaction between them with proteins expressed in vitro and by yeast two-hybrid tests were not successful. It thus appears likely that at least one additional linker protein may be required to associate mitochondria with this motor. A precedent for a protein complex serving as an adaptor exists in mLin2, mLin7, and mLin10, which form the probable adaptor for vesicles delivering NMDA receptors to dendrites (Setou et al., 2000). Alternatively, it remains possible that Milton is not the adaptor per se, but rather a protein that regulates independently bound Kinesin to the mitochondrion. Some kinesins, for example, may be bound via a combination of protein factors and direct interactions with membrane lipids (Klopfenstein et al., 2002). Furthermore, anti-KHC antibodies preferentially precipitate only a subset of Milton isoforms, suggesting that Milton may also function independently of KHC. Such roles could include tethering mitochondria at discrete energy-requiring locations within the nerve terminal or linking mitochondria to other kinesin-like motors. An indirect role for Milton in synaptic plasticity could arise from the involvement of mitochondria in regulating calcium concentrations in the nerve terminal (reviewed in Zucker, 1999), as discussed further below. Nonneuronal functions concerning mitochondrial movement or localization are also suggested by the early embryonic expression of Milton before neurons arise, which may reflect mitochondrial motility during cellularization.

Overexpression of a component of a dynein adaptor complex, dynamitin, exerts a dominant-negative effect on transport by dynein, disrupting retrograde axonal transport and causing cargoes to accumulate at the plus end of microtubules (Burkhardt et al., 1997). In this context, it is interesting to note that we observed a redistribution of the mitochondria in HEK293T cells when Milton was overexpressed; the mitochondria became tightly clustered in the vicinity of the Golgi apparatus, a structure associated with the minus ends of microtubules (Lippincott-Schwartz et al., 1995). The redistribution may result from a comparable inhibition of kinesin, the plus end-directed motor, causing the mitochondria to accumulate at the minus ends.

No discernible sequence motif or structural characteristic unites the adaptor proteins that have so far been identified. In addition to mLin2, mLin7, and mLin10, these include Sunday Driver, which functions on G58K-marked Golgi and post-Golgi vesicles (Bowman et al., 2000); related jun-interacting proteins (JIPs) that can bind vesicles via ApoER2 (Verhey et al., 2001); and β -1 adaptin, which is associated with post-Golgi vesicles bearing the mannose-6-phosphate receptor (Nakagawa et al., 2000). The observations that mitochondria move along axons at speeds similar to those of known kinesins (Morris and Hollenbeck, 1993) and that mitochondria accumulate in the axons of *Drosophila* with mutant kinesin heavy chain (Hurd and Saxton, 1996) together predict the existence of a mitochondria-specific kinesin-adaptor in neurons. However, no such mitochondrial protein has been identified.

Milton is the *Drosophila* protein showing greatest identity to HAP-1, suggesting that HAP-1 may serve a related function. Indeed there are noteworthy similarities between our findings and what is known about HAP-1. HAP-1 is expressed primarily in neurons (along axons and in nerve terminals [Li et al., 2000]), is transported up and down axons (Block-Galarza et al., 1997), and colocalizes with many, but not all, organelles including ER, synaptic vesicles, tubulovesicles, endosomes, and mitochondria, as well as with microtubules (Gutekunst et al., 1998). Moreover, HAP-1 binds to p150/Glued, a subunit of dynactin, and thus may be associated in turn with dynein (Engelender et al., 1997, Li et al., 1998).

It is likewise interesting that there are two Milton homologs in the human genome but none in the reported genomes of nematodes, plants, or yeast. In these species, no genes encode proteins with >25% identity to the coiled-coil region of Milton or any significant homology with the more highly conserved C-terminal homology region. These organisms lack the lengthy axons and complex cellular structures of arthropods and vertebrates and may not therefore need the active transport of mitochondria. The yeast tropomyosin 1 gene (*tpm1*; Hermann et al., 1997; Simon et al., 1997), shows 25% identity over 148 amino acids in the coiled-coil domain of Milton and exhibits a mitochondria distribution phenotype at cell division. Possibly, therefore, Milton evolved from a Tpm1-like protein to take on a role in axonal transport of mitochondria.

Dysfunctional Synaptic Transmission in the Absence of Mitochondria

The initial observation leading to the isolation of *milton*, that the behavior and ERG of flies with homozygous *milton* photoreceptors indicated a defect in transmission by photoreceptors to downstream neurons, must be a consequence of the pivotal finding that these *milton* photoreceptors lack mitochondria at their terminals. Precisely how the absence of mitochondria impairs signaling, however, is less certain. The otherwise surprisingly normal ultrastructure of *milt¹⁸⁶/milt¹⁸⁶* terminals implies that the physiological defect is not a symptom of degeneration at the terminal and that some metabolic needs of the terminal are apparently met by other energy sources such as anaerobic metabolism and the diffusion of ATP from the soma. Although the affected terminals

may possibly release some neurotransmitter, the extent or synchronization of any release must be sufficiently altered to result in poor phototaxis and the absence of on- and off-transients in the ERG.

Why, then, are *Drosophila* photoreceptor nerve terminals dysfunctional in the absence of mitochondria? The absence of mitochondria and consequent decrease in ATP supply could adversely affect any number of ATP-dependent processes in the terminal or axon including: the vesicular proton pump that provides the energy to load vesicles with neurotransmitter; the $\text{Na}^+/\text{Ca}^{2+}$ exchanger that extrudes Ca^{2+} from the nerve terminal; the Na^+/K^+ -ATPase; or NSF, which facilitates the vesicle cycle by dissociating SNARE proteins. Because the population of vesicles in the terminals is not severely depleted, energy-dependent steps of endocytosis, including dynamin-dependent fission or clathrin-uncoating, seem not to be greatly compromised.

Ca^{2+} homeostasis in the terminal may be particularly compromised by the absence of mitochondria. Not only will the extrusion of Ca^{2+} across the plasmalemma be diminished if the Na^+ gradient runs down, but additionally, given that mitochondria take up Ca^{2+} after a Ca^{2+} spike, the absence of mitochondria would increase residual cytosolic Ca^{2+} . This accumulation of Ca^{2+} could gradually increase neurotransmitter release even in the absence of stimulation. It is therefore possible that the absence of on- and off-transients in the ERG results not from an inability to release neurotransmitter, but rather from a constant release that is independent of light.

Our findings, that Milton is associated with Kinesin heavy chain and is required for axonal transport of mitochondria, now make it possible to address a number of questions. How does Milton attach to mitochondria and to Kinesin, and does Milton's attachment invariably destine a mitochondrion to be transported down the axon? How is the appropriate number of mitochondria in a nerve terminal established? Does nerve terminal activity alter the number of mitochondria present via Milton? It is hoped that the identification of Milton as an essential element of mitochondrial localization will make these questions accessible to biochemical study.

Experimental Procedures

Stocks and Mutagenesis

The *yw*; *FRT40A GMR-hid CL 2L/CyO*; *EGUF/EGUF* and *FRT40A syt^{AD4}* stocks were previously described (Stowers and Schwarz, 1999). The *FRT40A* chromosome (Xu and Rubin, 1993) and *Df (2L) J-H* were obtained from the Bloomington Stock Center. *milt^{(2) K14514}* and *milt^{(2) K06704}* were obtained from the Berkeley *Drosophila* Genome Project. Males isogenic for a *FRT40A* chromosome were fed 10 mM ethylmethylsulfonate in 1% sucrose for 8 hr and mated immediately. The frequency of X linked lethals was 0.2/chromosome. In total, approximately 3000 lethal mutations were screened. Lethal period was determined by crossing both *milt⁹²* and *Df (2L) J-H* into a *yw* background and using the *Cy0,y+* balancer chromosome.

Phototaxis Screening

Phototaxis screening was carried out using a phototaxis apparatus (Benzer, 1967) constructed to hold five removable 250 ml Erlenmeyer flasks (Nalgene 4104-0250) on each side. For the F_1 phototaxis screen, ≤ 500 flies were placed in each of five flasks wrapped with black masking tape and inserted on one side of the apparatus, agitated, and given approximately 30 s to move horizontally to the flasks on the opposite side, which had at their bases a fluorescent

light. Recombinant eye males that failed in two trials to leave the original flask were individually mated to virgin females of the genotype *yw; FRT40A GMR-hid CL 2L/CyO; EGF/EGUF*, and their recombinant eye progeny were rescreened for phototaxis in the F₂ generation. ERGs were performed on recombinant-eye flies from vials whose recombinant-eye populations showed poor phototaxis (Stowers and Schwarz, 1999), and stocks were established from those with aberrant on-/off-transients.

Generation of Antibodies

The Milton fusion proteins against which antibodies were made were generated as follows. For P1-152, an EcoRI/XhoI PCR fragment encoding amino acids 1–152 was inserted into the EcoRI/XhoI sites of pMalc (Pharmacia, Piscataway, NJ). For 2B30 and 2A108, an EcoRV/Sall fragment (amino acids 273–449) was inserted into the SmaI/XhoI sites of pGEX4T2 (New England Biolabs, Cambridge, MA). For 4A75, a Sall/StuI fragment (amino acids 752–901) was inserted into the Sall/NotI-blunt sites of pGEX4T2. For 5A124, an NruI/SfoI fragment (amino acids 908–1055) was inserted into the SmaI site of pGEX4T3.

Molecular Genetics

EcoRI digested DNA from line *K06704* was transformed into *E. coli*, and the rescued plasmid containing 5.5 kb of genomic DNA was used to isolate genomic phage #4 from a library (Tamkun et al., 1991). A 7 kb EcoRI/Sall genomic fragment was used to probe the Berkeley *Drosophila* Genome Project LD 0–24 hr embryonic cDNA library. Genomic phage #31 was isolated using as a probe a 1.7 kb BglII/XhoI fragment from the 3' end of the longest milton cDNA. The milton genomic rescue construct in pCasPeR contained ~22 kb of contiguous genomic DNA from the Sall site approximately 1.5 kb upstream of the putative milton 5' end to the BamHI site approximately 2.5 kb downstream of the milton 3' end (Figure 3A).

Immunohistochemistry

First instar larvae were dissected on Sylgard-coated slides using Nexaband glue to fix them to the surface, fixed in 4% paraformaldehyde for 10 min, blocked with PBS containing 5% NGS and 0.5% Triton X-100 (PBSNT) for 1 hr at room temperature (RT, approximately 23°C), incubated with primary antibody in PBSNT O/N at 4°C, washed three times in PBS, blocked with PBSNT for 1 hr at RT, and incubated with goat-anti-mouse Alexa-488 (Jackson) or goat-anti-rabbit Cy3 (Jackson) secondary antibodies. For fly head cryostat sections, flies were decapitated, their probosces removed, head capsules fixed in 4% paraformaldehyde in PBS for 2 hr at RT, and incubated in sucrose in PBS (5% for 10 min at RT, 10% for 10 min at RT, 25% O/N at 4°C). Heads were placed in OCT, frozen in liquid N₂, and 10 μm cryostat sections cut and air dried on slides for 30 min. Slides were then placed in 1 mM EDTA at 95°C for 5 min to unmask epitopes. For immunolabeling, mounted cryostat sections were processed as described above, except HRP-conjugated secondary antibodies (Jackson) were used and the slides developed with diaminobenzidine (Sigma) in 0.03% H₂O₂. Mouse anti-Chaoptin (24B10) (Fujita et al., 1982) was used at 1:100. Rabbit anti-Syt (Littleton et al., 1993) was used at 1:1000. Mouse anti-Milton antibodies were used at 1:10. Rabbit anti-Hsp60 (Morrow et al., 2000) was used at 1:1000. Rabbit anti-KHC (Cytoskeleton) was used at 1:1000.

HEK293T cells were cultured in DMEM supplemented with 10% fetal calf serum (FCS), L-glutamine, and penicillin-streptomycin. Cells were transfected via calcium phosphate either with full-length *milton* cDNA in pCMV (Stratagene) or without DNA (sham-transfected). To visualize mitochondria and transferrin receptors, cells were incubated with 100 nM MitoTracker Red for 15 min or 50 mg/ml transferrin-AlexaFluor 594 (Molecular Probes) for 30 min. For immunofluorescence, cells were washed in PBS, fixed in 4% paraformaldehyde/PBS for 15 min, and blocked with 0.1% FCS, 0.1% BSA, and 1% Triton in PBS. Primary antibodies were diluted in blocking solution or PBS and incubated with cells for 1–16 hr. After a PBS wash, secondary Cy3- or FITC-conjugated antibodies (Jackson) were diluted in PBS with 1% Tween, followed by PBS wash and fixation in –20°C methanol for 5 min. Cells were viewed with a 100/1.3 Nikon objective and images collected using Noran OZ Confocal software. In this study, mAb 2A108 (above) was used to

visualize Milton though similar results were observed with mAbs 4A75 and 5A124 (data not shown). Other antibodies used in this study include: rabbit anti-kinesin (Cytoskeleton), rabbit anti-TRAPa (gift of T.A. Rapoport), and rabbit anti-giantin (Covance).

EM

Scanning EM was performed as previously described (Stowers and Schwarz, 1999). For transmission EM, adult *mit⁹²* or *mit¹⁸⁶* mutant flies were obtained from the cross of *y,w; FRT 40, milton /CyO,y+* and *y,w; FRT 40, GMR-hid CL2L EGF/CyO,y+*. Control flies were obtained from the cross between *y,w; FRT 40A*, the parental chromosome stock, and *y,w; FRT 40, GMR-hidCL EGF/CyO,y+*. The heads of *mit* adult flies were bisected, immersed in a cacodylate-buffered paraformaldehyde and glutaraldehyde primary fixative, and processed for EM (Meinertzhagen and O'Neil, 1991). Ultrathin sections cut at 65 nm thickness were stained with uranyl acetate (10 min) and lead citrate (10 min). Counts of organelle profiles were made blind by a single observer and included three flies of each genotype.

Subcellular Fractionation

Fly heads were purified and stored at –70°C until use. All manipulations were at 4°C unless otherwise noted. Lysate for glycerol gradients (Figure 5C) was prepared by pulverizing heads in a liquid N₂ chilled mortar and homogenizing the powder in a 10× volume of buffer (150 mM NaCl, 10 mM HEPES [pH 7.4], 1 mM EGTA, 0.1 mM MgCl₂ containing protease inhibitors aprotinin 1 μg/ml, leupeptin 1 μg/ml, pepstatin 1 μg/ml, and PMSF 50 μg/ml). Postnuclear supernatant (10 min at 1000 g) was layered onto 5%–25% glycerol gradients in homogenization buffer and spun in a Beckman SW41 rotor at 197,000 g (38,000 rpm) for 2 hr (Figure 5C). Fractions were collected, equal volumes run on SDS-PAGE, and analyzed by immunoblot. For the sucrose gradient (Figure 5D), adult flies were homogenized in 0.25 M sucrose, 10 mM Tris (pH 7.5), 1 mM EDTA, and protease inhibitors as above. Postnuclear supernatant was loaded onto a 1–2 M sucrose gradient, spun at 55,000 g for 2 hr, and processed as above.

Mass Spectrometry

To precipitate Milton complexes from *Drosophila* head extracts, 2A108 and 5A124 were used separately. The precipitates were separated by SDS-PAGE and proteins visualized by silver staining. Specific coprecipitating protein bands were excised, digested with trypsin, and subjected to analysis by matrix-assisted laser desorption/ionization reflector time-of-flight (MALDI-TOF) mass spectrometry on a Perseptive Voyager-DE RP Biospectrometry instrument (Stanford University). The observed peptide masses were analyzed using ProFound software (<http://prowl.rockefeller.edu/cgi-bin/prot-id>). Anti-kinesin antibodies were provided by William Saxton (Indiana University) and purchased from Cytoskeleton, Inc. (Denver, CO).

Acknowledgments

We thank Dr. William Saxton for the generous gift of antibodies and flies, Matt Fish for embryo injections, and Mss. Irene Inman and Rita Kostyleva for expert technical assistance. Supported by NIH grants MH48108 and NS41062 (to T.L.S.), NS10561 (to R.S.S.), NS07473 (to L.J.M.), and EY03592 (to I.A.M.); and by the Killam Trust of Dalhousie University (to I.A.M.).

Received: June 29, 2001

Revised: October 23, 2002

References

- Benzer, S. (1967). Isolation of *Drosophila* behavioural mutants using countercurrent selection. *Proc. Natl. Acad. Sci. USA* 58, 1112–1119.
- Block-Galarza, J., Chase, K.O., Sapp, E., Vaughn, K.T., Vallee, R.B., DiFiglia, M., and Aronin, N. (1997). Fast transport and retrograde movement of huntingtin and HAP 1 in axons. *Neuroreport* 8, 2247–2251.
- Bowman, A.B., Kamal, A., Ritchings, B.W., Philp, A.V., McGrail, M., Gindhart, J.G., and Goldstein, L.S. (2000). Kinesin-dependent axonal

- transport is mediated by the Sunday driver (SYD) protein. *Cell* 103, 583–594.
- Brand, A.H., and Perrimon, N. (1993). Targeted gene expression as a means of altering cell fates and generating dominant phenotypes. *Development* 118, 401–415.
- Burkhardt, J.K., Echeverri, C.J., Nilsson, T., and Vallee, R.B. (1997). Overexpression of the dynamin (p50) subunit of the dynactin complex disrupts dynein-dependent maintenance of membrane organelle distribution. *J. Cell Biol.* 139, 469–484.
- Coombe, P.E., and Heisenberg, M. (1986). The structural brain mutant Vacuolar medulla of *Drosophila melanogaster* with specific behavioral defects and cell degeneration in the adult. *J. Neurogenet.* 3, 135–158.
- Engelender, S., Sharp, A.H., Colomer, V., Tokito, M.K., Lanahan, A., Worley, P., Holzbaun, E.L., and Ross, C.A. (1997). Huntingtin-associated protein 1 (HAP1) interacts with the p150Glued subunit of dynactin. *Hum. Mol. Genet.* 6, 2205–2212.
- Fujita, S.C., Zipursky, S.L., Benzer, S., Ferrus, A., and Shotwell, S.L. (1982). Monoclonal antibodies against the *Drosophila* nervous system. *Proc. Natl. Acad. Sci. USA* 79, 7929–7933.
- Goldstein, L.S., and Yang, Z. (2000). Microtubule-based transport systems in neurons: the roles of kinesins and dyneins. *Annu. Rev. Neurosci.* 23, 39–71.
- Gutkunst, C.A., Li, S.H., Yi, H., Ferrante, R.J., Li, X.J., and Hersch, S.M. (1998). The cellular and subcellular localization of huntingtin-associated protein 1 (HAP1): comparison with huntingtin in rat and human. *J. Neurosci.* 18, 7674–7686.
- Heisenberg, M. (1971). Separation of receptor and lamina potentials in the electroretinogram of normal and mutant *Drosophila*. *J. Exp. Biol.* 55, 85–100.
- Hermann, G.J., King, E.J., and Shaw, J.M. (1997). The yeast gene, MDM20, is necessary for mitochondrial inheritance and organization of the actin cytoskeleton. *J. Cell Biol.* 137, 141–153.
- Hollenbeck, P.J. (1996). The pattern and mechanism of mitochondrial transport in axons. *Front. Biosci.* 1, d91–d102.
- Hurd, D.D., and Saxton, W.M. (1996). Kinesin mutations cause motor neuron disease phenotypes by disrupting fast axonal transport in *Drosophila*. *Genetics* 144, 1075–1085.
- Kikuno, R., Nagase, T., Ishikawa, K., Hirose, M., Miyajima, N., Tanaka, A., Kotani, H., Nomura, N., and Ohara, O. (1999). Prediction of the coding sequences of unidentified human genes. XIV. The complete sequences of 100 new cDNA clones from brain which code for large proteins in vitro. *DNA Res.* 6, 197–205.
- Klopfenstein, D.R., Tomishige, M., Stuurman, N., and Vale, R.D. (2002). Role of phosphatidylinositol(4,5)bisphosphate organization in membrane transport by the Unc104 kinesin motor. *Cell* 109, 347–358.
- Langford, G.M. (1995). Actin- and microtubule-dependent organelle motors: interrelationships between the two motility systems. *Curr. Opin. Cell Biol.* 7, 82–88.
- Li, S.H., Gutkunst, C.A., Hersch, S.M., and Li, X.J. (1998). Interaction of huntingtin-associated protein with dynactin P150Glued. *J. Neurosci.* 18, 1261–1269.
- Li, S.H., Li, H., Torre, E.R., and Li, X.J. (2000). Expression of huntingtin-associated protein-1 in neuronal cells implicates a role in neurite growth. *Mol. Cell. Neurosci.* 16, 168–183.
- Li, X.J., Li, S.H., Sharp, A.H., Nucifora, F.C., Jr., Schilling, G., Lanahan, A., Worley, P., Snyder, S.H., and Ross, C.A. (1995). A huntingtin-associated protein enriched in brain with implications for pathology. *Nature* 378, 398–402.
- Ligon, L.A., and Steward, O. (2000). Movement of mitochondria in the axons and dendrites of cultured hippocampal neurons. *J. Comp. Neurol.* 427, 340–350.
- Lippincott-Schwartz, J., Cole, N.B., Marotta, A., Conrad, P.A., and Bloom, G.S. (1995). Kinesin is the motor for microtubule-mediated Golgi-to-ER membrane traffic. *J. Cell Biol.* 128, 293–306.
- Littleton, J.T., Bellen, H.J., and Perin, M.S. (1993). Expression of synaptotagmin in *Drosophila* reveals transport and localization of synaptic vesicles to the synapse. *Development* 118, 1077–1088.
- Meinertzhagen, I.A., and Hanson, T.E. (1993). The development of the optic lobe. In: *The Development of Drosophila Melanogaster* (Plainview, NY: Cold Spring Harbor Laboratory Press), pp. 1363–1491.
- Meinertzhagen, I.A., and O’Neil, S.D. (1991). Synaptic organization of columnar elements in the lamina of the wild type in *Drosophila melanogaster*. *J. Comp. Neurol.* 305, 232–263.
- Meinertzhagen, I.A., and Sorra, K.E. (2001). Synaptic organization in the fly’s optic lamina: few cells, many synapses and divergent microcircuits. *Prog. Brain Res.* 131, 53–69.
- Meinertzhagen, I.A., Piper, S.T., Sun, X.J., and Fröhlich, A. (2000). Neurite morphogenesis of identified visual interneurons and its relationship to photoreceptor synaptogenesis in the flies, *Musca domestica* and *Drosophila melanogaster*. *Eur. J. Neurosci.* 12, 1342–1356.
- Morris, R.L., and Hollenbeck, P.J. (1993). The regulation of bidirectional mitochondrial transport is coordinated with axonal outgrowth. *J. Cell Sci.* 104, 917–927.
- Morrow, G., Inaguma, Y., Kato, K., and Tanguay, R.M. (2000). The small heat shock protein Hsp22 of *Drosophila melanogaster* is a mitochondrial protein displaying oligomeric organization. *J. Biol. Chem.* 275, 31204–31210.
- Nagase, T., Ishikawa, K., Miyajima, N., Tanaka, A., Kotani, H., Nomura, N., and Ohara, O. (1998). Prediction of the coding sequences of unidentified human genes. IX. The complete sequences of 100 new cDNA clones from brain which can code for large proteins in vitro. *DNA Res.* 5, 31–39.
- Nakagawa, T., Setou, M., Seog, D., Ogasawara, K., Dohmae, N., Takio, K., and Hirokawa, N. (2000). A novel motor, KIF13A, transports mannose-6-phosphate receptor to plasma membrane through direct interaction with AP-1 complex. *Cell* 103, 569–581.
- Nangaku, M., Sato-Yoshitake, R., Okada, Y., Noda, Y., Takemura, R., Yamazaki, H., and Hirokawa, N. (1994). KIF1B, a novel microtubule plus end-directed monomeric motor protein for transport of mitochondria. *Cell* 79, 1209–1220.
- Pereira, A.J., Dalby, B., Stewart, R.J., Doherty, S.J., and Goldstein, L.S. (1997). Mitochondrial association of a plus end-directed microtubule motor expressed during mitosis in *Drosophila*. *J. Cell Biol.* 136, 1081–1090.
- Peters, A., Palay, S.L., and Webster, H.D. (1991). *The Fine Structure of the Nervous System: The Neurons and Supporting Cells* (New York: Oxford University Press).
- Setou, M., Nakagawa, T., Seog, D.H., and Hirokawa, N. (2000). Kinesin superfamily motor protein KIF17 and mLin-10 in NMDA receptor-containing vesicle transport. *Science* 288, 1796–1802.
- Simon, V.R., Karmon, S.L., and Pon, L.A. (1997). Mitochondrial inheritance: cell cycle and actin cable dependence of polarized mitochondrial movements in *Saccharomyces cerevisiae*. *Cell Motil. Cytoskeleton* 37, 199–210.
- Stowers, R.S., and Schwarz, T.L. (1999). A genetic method for generating *Drosophila* eyes composed exclusively of mitotic clones of a single genotype. *Genetics* 152, 1631–1639.
- Stürmer, K., Baumann, O., and Walz, B. (1995). Actin-dependent light-induced translocation of mitochondria and ER cisternae in the photoreceptor cells of the locust *Schistocerca gregaria*. *J. Cell Sci.* 108, 2273–2283.
- Tamkun, J.W., Kahn, R.A., Kissinger, M., Brizuela, B.J., Rulka, C., Scott, M.P., and Kennison, J.A. (1991). The arflike gene encodes an essential GTP-binding protein in *Drosophila*. *Proc. Natl. Acad. Sci. USA* 88, 3120–3124.
- Tanaka, Y., Kanai, Y., Okada, Y., Nonaka, S., Takeda, S., Harada, A., and Hirokawa, N. (1998). Targeted disruption of mouse conventional kinesin heavy chain, kif5B, results in abnormal perinuclear clustering of mitochondria. *Cell* 93, 1147–1158.
- Vallee, R.B., and Sheetz, M.P. (1996). Targeting of motor proteins. *Science* 271, 1539–1544.
- Verhey, K.J., Meyer, D., Deehan, R., Blenis, J., Schnapp, B.J., Rapoport, T.A., and Margolis, B. (2001). Cargo of kinesin identified as JIP

scaffolding proteins and associated signaling molecules. *J. Cell Biol.* *152*, 959–970.

Werth, J.L., and Thayer, S.A. (1994). Mitochondria buffer physiological calcium loads in cultured rat dorsal root ganglion neurons. *J. Neurosci.* *14*, 348–356.

Wong-Riley, M.T., and Welt, C. (1980). Histochemical changes in cytochrome oxidase of cortical barrels after vibrissal removal in neonatal and adult mice. *Proc. Natl. Acad. Sci. USA* *77*, 2333–2337.

Xu, T., and Rubin, G.M. (1993). Analysis of genetic mosaics in developing and adult *Drosophila* tissues. *Development* *117*, 1223–1237.

Zhao, C., Takita, J., Tanaka, Y., Setou, M., Nakagawa, T., Takeda, S., Yang, H.W., Terada, S., Nakata, T., Takei, Y., et al. (2001). Charcot-marie-tooth disease type 2a caused by mutation in a microtubule motor kif1bbeta. *Cell* *105*, 587–597.

Zucker, R.S. (1999). Calcium- and activity-dependent synaptic plasticity. *Curr. Opin. Neurobiol.* *9*, 305–313.

Accession Numbers

The GenBank accession numbers of the 5.2 kb and 4.2 kb *milton* mRNAs are AY038000 and AY038001, respectively.